1-1-2009

Experimental Evidence of Non-Linear Dissipation Using Acoustic Micro-Lapses

G. Quiroga-Goode
Universidad Autonóma de Tamaulipas

K. van Wijk
Boise State University

Experimental Evidence of Non-Linear Dissipation Using Acoustic Micro-Lapses

G. QUIROGA-GOODE and K. VAN WIJK

ABSTRACT

Non-linear material behaviour is observed experimentally in a laboratory using a new method called Acoustic Micro-Lapses (AML). In this approach, the shooting of two waves is synchronised in a way that the second wave (TW) is to sense the fluctuations in material stiffness induced by the first (PW). The tests include four samples; twenty trials are performed for each sample by increasing time-delays between the waves. The recorded waves are decoupled and compared to determine spectral differences by computing a quantity proportional to the energy difference as function of the increasing time delay ($E^{m}_{\Delta t}$). For a tight sandstone and aluminium samples, the random behaviour of $E^{m}_{\Delta t}$ implies that TW finds the same equilibrium conditions as PW. The Lucite and the Berea sandstone depict distinct maxima, implying that TW sensed the transitory perturbations induced by PW. Therefore, it is inferred that PW and TW must propagate with different phase speeds.

To assess the previous results, quasi-static modelling is performed using two time delayed step functions. The corresponding creep compliance shows a strong discontinuity when the second step is applied, implying the existence of two unrelaxed moduli. This supports the lab data in that the two waves must have different dispersion relations such that they propagate with different speeds.

METHOD

It is presented the results of a new method called Acoustic Micro-Lapses (AML) aimed at material characterization. It consists of sequentially shooting two seismic wavefields separated by a time delay. The second field, called Tracking Wave (TW) is to probe the transient fluctuations of the medium stiffness induced by the acoustic excitation of the first, called Pilot Wave (PW). The synchronized shooting of PW and TW can be thought of as sending a single composite wavefield whose phase has been modulated; any further changes in the prescribed phase can be attributed to changes in the material properties associated to non-linear

G. Quiroga-Goode, Inst. Inv. Ing., Universidad Autónoma de Tamaulipas, Tampico, México
Kasper Van Wijk, Physical Acoustics Lab, Geosciences Dept., Boise State University, USA

dissipative effects. While the linear theories of viscoelasticity or poroelasticity allow material stiffness to vary with time, linearity implies that TW and PW cannot interact, i.e., both will find the same equilibrium conditions. In other words, material deformations are recovered instantly and thus, PW and TW will have the same spectra. Thus, it is only when the medium deforms non-linearly, that TW and PW will propagate with different spectral properties. This approach is similar to [1,2] in that two high-frequency wavefields are used to characterizing materials.

ULTRASONIC TESTING

The laboratory experiments were done at the Physical Acoustics Laboratory of Colorado School of Mines. The equipment comprises a 100 MHz pulser (Tektronix AFG) , a 200 MHz Oscilloscope (DPO) and two piezoelectric 0.5 MHz transducers.

Four cylindrical samples are considered of different rheologies. They are 7-13 cm long and a few cms in diameter. They correspond to porous sandstones: Lyon (1% porosity and permeability K=1 mD) and Berea (23.5 % porosity and permeability K=0.782 D). It is also considered solid samples of Lucite and aluminium. All are semi-dry and the tests were carried out at room temperature. An additional test involves heating the Berea sandstone.

Experimental Procedure

The procedure involves three steps. In the first two waveforms (PW and TW) are linearly superposed; they are separated by a time-shift Δt. The frequency and amplitude of each wave is the same: $S(t) = \sin(2\pi t/T_0) - 0.5\sin(4\pi t/T_0)$, $0<t<T_0^{-1}$ where T_0 corresponds to the dominant wave period; S(t) can have any form. Therefore, the superposition of the waves results in a composite signal whose phase has been modulated; this composite wave is called $PTW_{\Delta t}$.

In the second step, $PTW_{\Delta t}$ is input into the sample via the transducer using the pulser and recorded in the oscilloscope after passing through the second transducer. Since the particular time delay or delays at which the TW could sense the transient oscillations of the stiffness induced by PW is unknown, the previous test is repeated several times, each having an increasing delay: $\Delta t=0:dt:T_0$. This notation means that the time shifts Δt start at 0, end at T_0 and have a time step Δt; at $\Delta t=0$, the PW and TW are in phase and at $\Delta t=T_0$, they are fully out of phase. The recorded waveforms are termed $PTW^*_{\Delta t}$; the star denotes that the waves have been filtered after propagating through the sample. Only transmission effects are analyzed. Parameter Δt is a multiple of the time sampling step in the recordings. The oscilloscope is programmed to stack 512 recordings in approximately 4 s to improve the S/N.

To assess if TW sensed any transient perturbations induced by PW in the recorded composite signal $PTW^*_{\Delta t}$, in the next step PW is fed alone through the sample. Then it is computed $TW^{**}_{\Delta t} = PTW^*_{\Delta t} - PW^*$ for $\Delta t=0:dt:T_0$; double star means that TW has been obtained by decoupling it from $PTW^*_{\Delta t}$. Thus, in the last step, the differences between PW and TW are computed for each of the twenty time delays and for each of the material samples as follows:

$$E_{\Delta t}^{m} = \sum_{n=1}^{k} \left(PW_{n}^{*} - TW_{n-\Delta t}^{**} \right)^{2}, \quad \Delta t = 0{:}dt{:}T_{0} \tag{1}$$

where subscript 'n' represents the sample number in the recording and 'k' corresponds to the total number of samples in the recordings; k=16000 and Δt=5 μs. All samples in $TW_{n-\Delta t}^{**}$ are shifted back by an amount Δt to make PW and TW 'in phase'. Any further changes to the phase can be attributed to non-linearities. Therefore, $E_{\Delta t}$ represents a quantity proportional to the differential energy between the two waveforms as a function of time delay Δt. To remove the bias due to the materials having different compressibilities, $E_{\Delta t}$ is normalized to unity.

It is noted that PW^{*}, $PTW_{\Delta t}^{*}$ and $TW_{\Delta t}^{*}$ each actually represent a wave packet made up by the superposition of several wave types, including surface waves, direct waves, refractions, diffractions, internal reflections, etc. However, $E_{\Delta t}$ should not be affected since all waves types composing each packet are present in $PW_{\Delta t}^{*}$, $PTW_{\Delta t}^{*}$ and $TW_{\Delta t}^{*}$.

Experimental Results

In Figs. 1a-e are shown the recordings obtained of the four core samples for particular time-shifts between the PW and TW. The major amplitude differences in the coda are observed for the heated Berea sample.

In Fig. 2 it is plotted $E_{\Delta t}^{m}$ showing the net differences between PW and TW as a function of Δt for each of the core samples. Therefore, every point in each of the curves represents the sum of the squared difference between PW and TW for a given time delay. In principle, at Δt=0, the PW and TW are 'in phase', thus $E_{\Delta t} \equiv 0$. However, as will be seen, there are still some differences, which could be attributed to non-linearities and also to experimental errors; however it should be expected them to behave randomly. Therefore, significance can be drawn only when $E_{\Delta t}^{m}$ shows consistently maxima.

That function $E_{\Delta t}^{m}$ has different amplitudes for each material sample is related to difference in material compressibilites. As observed in this plot, the differences between PW and TW for the aluminum sample (pink) are random, as expected, since the material behaves linearly elastic. The same occurs with the Lyon sandstone (green), since it is compact and mostly filled with air. From the results obtained from Berea sandstone (dash blue), $E_{\Delta t}^{m}$ increases slightly as a function of time delay; a maximum is found at around 30 μs, after which it decreases uniformly. The previous scenario is changed when testing the Berea sandstone heated, as can be observed in the plot; there is a range of time shifts for which $E_{\Delta t}^{m}$ is largest. It should be remembered that the heating was done overnight and the sample tested the following day immediately after removing it from the oven. Thus the heat was dissipating as the testing was executing. The cooling off of the sample can be clearly correlated to $E_{\Delta t}^{m}$ decreasing with increasing Δt.

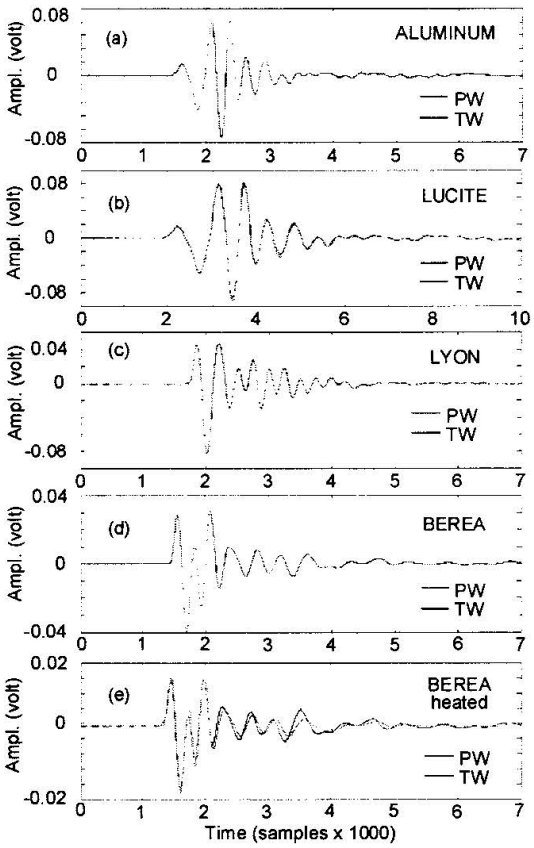

Figure 1. Recordings for the different samples at a particular Δt.

The last experiment is carried out with the Lucite sample, which is well known for its large attenuation at high frequencies. As can be seen in the graphics, there is a small range of 'Δt' for which the difference between the PW and TW is largest.

QUASI-STATIC MODELLING

A series of quasi-static numerical tests are carried out to shed light on the results obtained from the previous laboratory experiments. Among several theoretical models, the Standard Linear Solid (SLS) can be used to estimate the output strain

$$\varepsilon = \sigma_0 / E_1 + \sigma_0 (1 - e^{-t/\tau'})/E_2 \qquad (2)$$

to an input step-stress σ_0; this is called creep test. In this case, the subject sample reacts instantaneously as σ_0/E_1 and then the deformation increases asymptotically according to $\sigma_0(1 - e^{-t/\tau'}) /E_2$. Here t represents time, E_1 and E_2 are the physical parameters of the material (unrelaxed moduli). In this case, the model has a single relaxation mechanism. The corresponding retardation time τ' is given by $\tau' = \eta / E_2$.

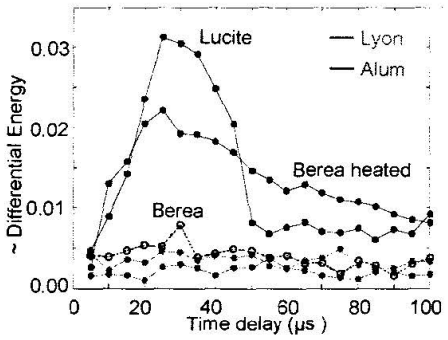

Figure 2. $E^{m}_{\Delta t}$ as a function of time delay Δt for different core samples. It represents a quantity proportional to the differential energy between the waves.

Here, η represents the material viscosity. Applying the hereditary law, i.e., Boltzman superposition principle, the composite strain due to a history of loading $\sigma = \sigma_0 + \sigma_1$ is given by $\varepsilon(t) = \sigma_0 J(t) + \Delta \sigma_1 J(t)$, where $J(t)=\varepsilon(t)/\sigma(t)$ corresponds to the Creep Compliance. The stress loads are shifted by amount t_s, as can be seen in Fig. 3. Creep Compliance is the quantity sought after since, being the inverse of the material stiffness, it will tell whether the second stress load will find different initial conditions than the first. However, while it is straightforward to compute the composite strain due to a history of loading, to extend the definition of Creep Compliance for multiple loads may not be as accurate.

It is shown in Fig. 3 the sequential application of two step stresses separated by a time-shift (t_s=0.3 ms). The model parameters are $E_1 = 1\text{x}10^9$ Pa, $E_1 = 5\ E_1$, $E_r = 5\text{x}10^{10}$ Pa, $\sigma_1=\sigma_2= 2\text{x}10^7$ Pa, $\eta = 1\text{x}10^{11}$ N s/m^2 and $\tau = 1\text{x}10^{-4}$ s.

In this case, the creep compliance (3c) develops a discontinuity when the second load is applied. In principle, the discontinuous curve presents two unrelaxed moduli. In the fully dynamic case that may imply that the two waves would have slightly different dispersion spectra, i.e., as if they propagate through slightly different media. In another example, not shown here, two step stresses are applied simultaneously, i.e., t_s=0 ms. In this case however, the creep compliance depicts a continuous increase in magnitude vs. time, as expected.

ANALYSIS AND CONCLUSIONS

A new method for material characterization is applied to probe the non-linear dissipative behaviour of materials. To determine its validity, it is quantified the spectral differences of the two waves. Since the relation between the amount of time delay and the non-linear behaviour is unknown, the tests are performed for several time-shifts: from zero to a maximum represented by the wave period.

The experimental results from the laboratory tests show that the aluminum and the compact Lyon porous sandstone behave overall linearly. While the Berea sandstone at room temperature picked up some small-magnitude non-linearity for a specific time delay, the heated test increased the effect significantly. There is a clear correlation between the cooling off of the sample with the decrease of this effect. The lucite also showed a large non-linear effect for a narrower range of Δt's.

To investigate the source of this behaviour, we modelled a SLS in the quasistatic regime. The computed creep compliance shows two distinct unrelaxed moduli, for each of the applied step functions. By inference, this implies that in the dynamic (ultrasonic) range, the two waves must have slightly different spectra, which is what the TW picked up.

It is noted that the process of stacking during the recording of the signals to improve the S/N could have masked the sought effect since it is time dependent. Since 512 recordings are stacked in less than 4 secs, it means that each signal is stacked in approximately 7.8 ms, assuming the stacking process were linear. The maximum time-delay between PW and TW during the testing was 0.1 ms, almost two orders of magnitude smaller than the stacking of each signal by the oscilloscope. Therefore, in principle it should not mask the non-linear effect of the material.

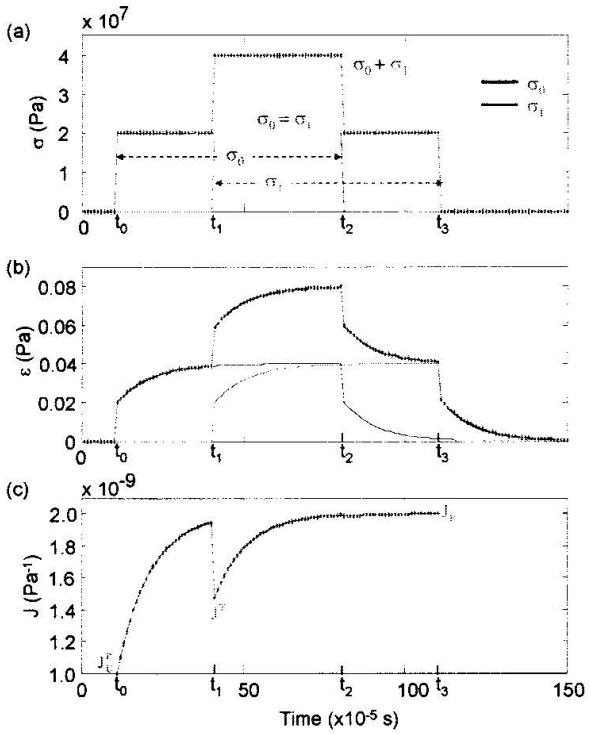

Figure 3. Mechanical response due to a composite loading. (a) Single (green and blue) and composite (red) stress loads, single (green and blue) and composite (red) strains (b) and composite creep compliance (c).

References

1. Khan, T. (2002). Elastic nonlinearity measurements help map permeability, pore fluids, Oil and Gas J., 100, p. 28.
2. Westervelt, P. J. (1963). Parametric Acoustic Array. J. Acoust. Soc. Am. 35, 535–537.